PAPER

# Adaptive Prediction Iterative Channel Estimation for Combined Antenna Diversity and Coherent Rake Reception of Multipath-Faded DSSS Signals

**Shinsuke TAKAOKA**†, ***Student Member and*** **Fumiyuki ADACHI**†, ***Regular Member***

**SUMMARY** Adaptive prediction iterative channel estimation is presented for combined antenna diversity and coherent rake reception of direct sequence spread spectrum (DSSS) signals. Its first stage uses pilot-aided adaptive prediction channel estimation, while the succeeding iteration stages use decision feedback and moving average filtering for channel re-estimation. The bit error rate (BER) performance of DSSS signal computer simulations evaluate transmission in a frequency selective Rayleigh fading channel. It is found that the adaptive prediction iterative channel estimation is superior to the non adaptive iterative channel estimation using the conventional weighted multi-slot averaging (WMSA) filtering at the first iteration stage, particularly in a fast fading channel.

***key words:*** *iterative channel estimation, pilot symbol, DSSS, fading channel*

## 1. Introduction

In mobile radio communications, the received signal experiences multipath fading, which is produced by interference of many waves having different Doppler shifts created by reflections and reflections by nearby buildings surrounding a mobile station [1]. The maximum Doppler shift of the faded signal becomes as high as 185 Hz for a carrier frequency of 2 GHz and a mobile user's traveling speed of 100 km/h. For coherent detection of received signals, channel estimation is necessary. To perform coherent detection in such a fast fading channel, pilot-aided channel estimation was proposed [2], [3], which uses periodically transmitted pilot symbols to estimate the instantaneous complex-valued gain of the fading channel. In the fast fading channel, the channel gain varies rapidly. To cope with fast fading, first and second order Gaussian interpolation methods can be used [3], [4]. Recently, a pilot-aided channel estimation called weighted multi-slot averaging (WMSA) channel estimation was proposed for coherent rake reception of direct sequence code division multiple access (DS-CDMA) cellular communications system [5].

The WMSA channel estimation consists of the following two steps. Pilot symbol block is time-multiplexed onto the data symbol sequence to be transmitted. In the first step, the instantaneous channel gain at the center time position of each pilot block is estimated by coherent addition of pilot symbols in the block. Then, at the second step, the $2K$ instantaneous channel gains are input to a $2K$-tap FIR filter to estimate the channel gain at each data symbol position in the data slot of interest. In [5], the $2K$ tap weights are optimized based on computer simulations. $K = 1$ WMSA is equivalent to a channel estimation using simple average of two pilot blocks belonging to the beginning and end of the data slot of interest [6]. Using the time invariant tap-weights cannot always minimize the bit error rate performance (BER) in changing fading environment due to user's movement. An adaptive updating method of the tap weights was proposed in [7], [8].

To further improve channel estimation, the number of pilot symbols needs to be increased; but the transmit power efficiency degrades. Decision feedback channel estimation can be used to increase the equivalent number of pilot symbols [9], [10]. Since combined data (by feedback) and pilot-aided channel estimation well matches a signal detection with iterative structure, this is employed for multistage interference cancellation [11], [12]. Of course, channel estimation itself can incorporate iterative structure. Recently, iterative channel estimation was applied to each stage of multistage interference cancellation [13]. Another example is a 2-stage receiver, in which predictive or non predictive channel estimation is first applied to make tentative decision and then, re-channel estimation based on the decision feedback of tentative decisions and removing data-modulation from the received signal samples is applied for better channel estimation [14]. Incorporating an iterative structure can extend this 2-stage receiver to a receiver with iterative channel estimation.

In this paper, adaptive prediction iterative channel estimation is presented for combined antenna diversity and coherent rake reception of direct sequence spread spectrum (DSSS) signals. The first iteration stage uses a pilot-aided adaptive prediction [8] and the second and later iteration stages use decision feedback and moving average filtering. The remainder of this paper is organized as follows. A transmission system with the adaptive prediction iterative channel estimation is

Manuscript received November 13, 2001.
Manuscript revised May 16, 2002.

†The authors are with Electrical and Communication Engineering, Graduate School of Engineering, Tohoku University, Sendai-shi, 980-8579 Japan.

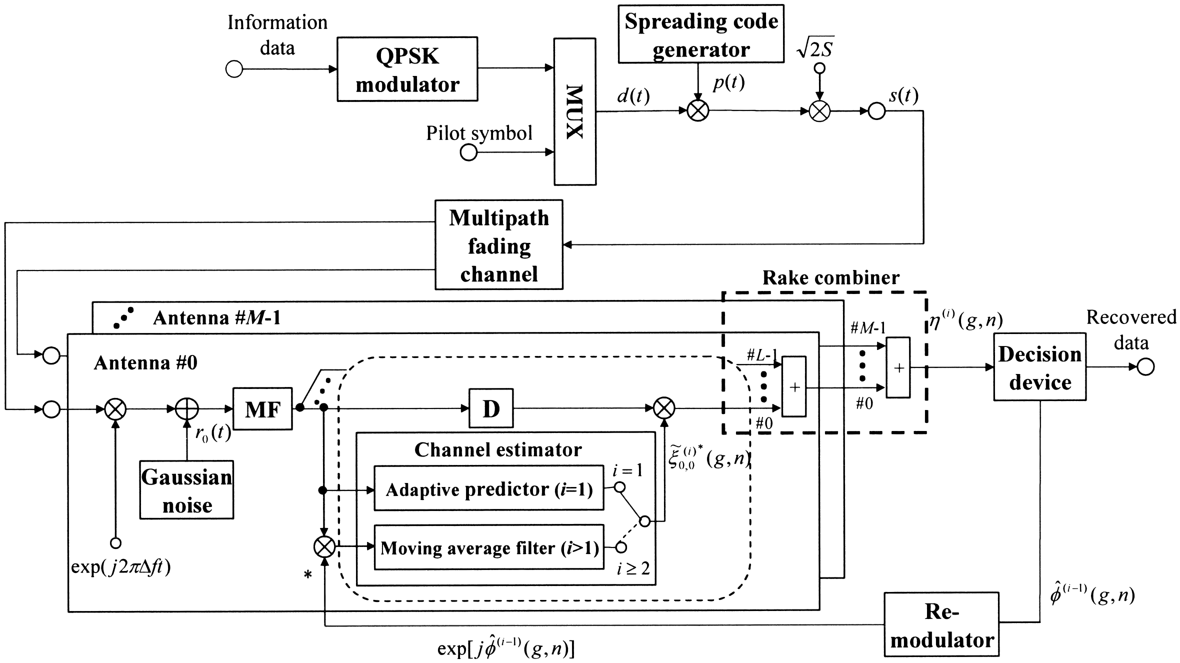


**Fig. 1** Transmission system in equivalent baseband representation.

described in Sect. 2. Section 3 presents the computer simulation results on combined antenna diversity and coherent rake reception of faded DSSS signals in a frequency selective Rayleigh fading channel and compares to a non-adaptive iterative channel estimation using the conventional WMSA filtering at the 1st iteration stage. Also considered is the channel estimation in the presence of frequency offset $\Delta f$ between the transmitter and receiver. Section 4 concludes the paper.

## 2. Transmission System Model and Adaptive Prediction Iterative Channel Estimation

A transmission system model is illustrated in Fig. 1. In what follows, the transmitter, propagation channel model, receiver and iterative channel estimation are described.

### 2.1 Transmitter

A binary transmission data is transformed into quaternary phase shift keying (QPSK)-modulated symbol sequence. Then, the known $N_p$ pilot symbols are time-multiplexed every $N_d$ data symbols as shown in Fig. 2. $N_p$ pilot symbols and succeeding $N_d$ data symbols make a slot with a length of $T_{slot} = (N_p + N_d)T$, where $T$ denotes QPSK symbol length. Finally, a spreading sequence is multiplied to the pilot-inserted QPSK symbol sequence to produce DSSS signal.

The DSSS signal $s(t)$ can expressed in a baseband equivalent representation as

$$s(t) = \sqrt{2S}d(t)p(t) \tag{1}$$

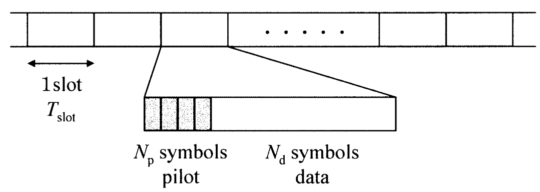


**Fig. 2** Slot structure.

with

$$\begin{cases} d(t) = \displaystyle\sum_{k=-\infty}^{\infty} \exp[j\phi(k)]u(t/T-k) \\ p(t) = \displaystyle\sum_{q=-\infty}^{\infty} c(q)u(t/T_c-q) \end{cases}, \tag{2}$$

where $S$ denotes the average signal power, $d(t)$ represents the QPSK symbol sequence waveform, and $p(t)$ the spreading sequence waveform. In Eq. (2), $\{c(q)\}$ represents the long random binary spreading sequence with chip length of $T_c$, $\phi(k) = \{(2m+1)\pi/4;\ m = 0 \sim 3\}$ is the QPSK-modulation phase, and $u(t)$ is the rectangular pulse with $u(t) = 1$ $(0 \leq t < 1)$ and 0 (otherwise), i.e., a rectangular chip pulse shaping is assumed without loss of generality. The spreading factor (SF) is given by $\mathrm{SF} = T/T_c$.

### 2.2 Propagation Channel Model

The DSSS signal is transmitted via a propagation channel. It is assumed that the propagation channel is frequency selective and has $L$ discrete paths having different time delays of multiple $T_c$ and experiencing independent Rayleigh fading. The receiver has a total of $M$ spatially separated antennas. The channel impulse response $h_m(t,\tau)$, seen on the $m$th antenna, $m = 0, 1, \ldots, M-1$, can be expressed as [16]

$$h_m(t,\tau) = \sum_{l=0}^{L-1} \xi_{m,l}(t)\delta(\tau - \tau_l), \tag{3}$$

where $\xi_{m,l}(t)$ and $\tau_l$ denote the complex fading channel gain and time delay of the $l$th path, respectively, with $E[\sum_{l=0}^{L-1} |\xi_{m,l}(t)|^2] = 1$, with E[.] being ensemble average operation. It is assumed that $\{\xi_{m,l}(t)\}$ are independent identically distributed (iid) complex Gaussian processes. The complex channel gain $\xi_{m,l}(t)$ time-varies, the received signal suffers from random phase variations (known as random FM noise [1]) and the random phase due to fading is uniformly distributed over $(-\pi, +\pi)$.

### 2.3 Receiver

The received signal $r_m(t)$ on the $m$th antenna can be expressed as

$$\begin{aligned} r_m(t) &= \sum_{l=0}^{L-1} r_{m,l}(t) + n_m(t) \\ &= \sum_{l=0}^{L-1} \xi_{m,l}(t)s(t-\tau_l) + n_m(t), \end{aligned} \tag{4}$$

where $n_m(t)$ denotes the additive white Gaussian noise (AWGN) with power spectrum density of $N_0$. The received faded DSSS signal is resolved into $L$ copies of transmitted QPSK symbol sequence by a matched filter (MF). The MF consists of $L$ correlators; each correlator multiplies $r_m(t)$ with the locally generated spreading sequence waveform $p(t)$, which is time-synchronized to the time delay of each propagation path, and integrates over one symbol period. In this paper, it is assumed that the receiver has the perfect knowledge of time delays of all propagation paths and that the receiver sampling timing is ideal. The MF output is sampled at the symbol rate. The MF output $r_{m,l}(g,n)$ at the $n$th symbol time epoch of the $g$th slot, associated with the $l$th path, is represented as

$$\begin{aligned} r_{m,l}(g,n) &= \frac{1}{T}\int_{gT_{slot}+nT+\tau_l}^{gT_{slot}+(n+1)T+\tau_l} r_m(t)p(t-\tau_l)dt \\ &= \sqrt{2S}\xi_{m,l}(g,n)\exp[j\phi(g,n)] \\ &\quad + w_{m,l}(g,n), \end{aligned} \tag{5}$$

where, $\xi_{m,l}(g,n) = \xi(gT_{slot} + nT)$, $\phi(g,n) = \phi(g(N_p + N_d) + n)$, and $w_{m,l}(g,n)$ represents the noise component.

A total of $M \times L$ MF outputs are coherently summed up based on maximal ratio combining (MRC) [1]. Denoting the channel estimate at the $i$th iteration stage as $\tilde{\xi}^{(i)}_{m,l}(g,n)$, the rake combiner output $\eta^{(i)}(g,n)$ can be represented as

$$\eta^{(i)}(g,n) = \sum_{m=0}^{M-1}\sum_{l=0}^{L-1} r_{m,l}(g,n)\tilde{\xi}^{(i)*}_{m,l}(g,n), \tag{6}$$

which is the decision variable at the $i$th iteration stage, where * denotes the complex conjugate.

### 2.4 Iterative Channel Estimation

The first iteration stage uses the pilot-aided adaptive prediction channel estimation to obtain $\tilde{\xi}^{(1)}_{m,l}(g,n)$. For the operation principle of the adaptive prediction channel estimation used in the first stage, see Appendix. The succeeding iteration stages use decision feedback and moving average filtering to obtain $\tilde{\xi}^{(i)}_{m,l}(g,n)$, $i > 1$. In the $i(> 1)$th iteration stage, the tentative decisions $\{\hat{\phi}^{(i-1)}(g,n)\}$ obtained at the previous iteration stage, i.e., the $(i-1)$th iteration stage, are fed back as pilot symbols to remove data modulation from the received MF output samples $\{r_{m,l}(g,n)\}$. The data-modulation removed received signal sample $\hat{\xi}^{(i)}_{m,l}(g,n)$ is given by

$$\hat{\xi}^{(i)}_{m,l}(g,n) = r_{m,l}(g,n)\exp[-j\hat{\phi}^{(i-1)}(g,n)], \tag{7}$$

Moving average filtering is applied to $\{\hat{\xi}^{(i)}_{m,l}(g,n)\}$ for channel re-estimation. The channel estimate at the $n$th symbol of the $g$th slot is obtained as

$$\tilde{\xi}^{(i)}_{m,l}(g,n) = \frac{1}{2Q+1}\sum_{j=-Q}^{Q} \hat{\xi}^{(i)}_{m,l}(g,n+j), \tag{8}$$

where the moving average interval is $2Q+1$ symbols, which is much longer than that of the first iteration stage; therefore, accuracy of channel estimation improves as the number of iterations increases.

## 3. Performance Evaluation

### 3.1 Computer Simulation Condition

The simulation condition is summarized in Table 1. The spreading sequence is a long PN sequence of $2^{12}-1$ chip period and the spreading factor is 64 chips per QPSK symbol. We use $N_p = 4$ and $N_d = 60$ and assume a frequency-selective Rayleigh fading channel with $L = 2$ paths. The first iteration stage uses the $K = 4$ pilot-aided adaptive prediction channel estimation [8]. For comparison, non-adaptive WMSA channel estimation filters using $K = 1$, 2, and 3 were also assumed in the first iteration stage; the tap weight vectors for $K = 1$, 2 and 3 are [1.0, 1.0], [0.6, 1.0, 1.0, 0.6] and [0.3, 0.8, 1.0, 1.0, 0.8, 0.3], respectively [5].

First, we consider the case without the frequency offset $\Delta f$ between the transmitter and receiver. The impact of the frequency offset is discussed in Sect. 3.6.

### 3.2 Optimization of Moving Average Filtering

Figure 3 plots the BER after the 2nd iteration ($i = 2$), with $f_D T_{slot}$ as a parameter, as a function of the moving average interval ($2Q + 1$ symbols) in the second iteration stage. The 3rd step of the 1st iteration stage uses simple averaging (SA) and linear interpolation (LI). In the figure, the BER curves labeled AP+SA(LI) are for adaptive prediction iterative channel estimation using SA (LI). In a slow fading channel, i.e., $f_D T_{slot} = 0.0064$, the BER monotonically reduces as the moving average interval for channel re-estimation used in the later stages increases. However, in a fast fading channel, i.e., $f_D T_{slot} = 0.32$, the BER first decreases and then, increases as the moving average interval increases. This is because the channel gain tends to vary within the moving average interval and the channel estimation error becomes larger. It is also seen from Fig. 3 that SA provides smaller BER in a slow fading channel; but, in a fast fading channel, it is LI that provides smaller BER. Since a moving average interval of $2Q + 1 = 101$ symbols overall achieves minimum BER, we use $Q = 50$ symbols in the following simulations.

**Table 1** Simulation condition.

| | | | |
|---|---|---|---|
| Transmitter | Spreading factor | 64 | |
| | Spreading sequence | Long random sequence | |
| | Modulation | Data | QPSK |
| | | Spreading | BPSK |
| | Slot structure | Pilot symbols: $N_p$=4<br>Information symbols: $N_d$=60 | |
| Channel model | Equal power 2-path Rayleigh fading | | |
| Receiver | Diversity | 2-branch antenna diversity($M$=2) + 2-finger rake($L$=2) | |

### 3.3 Channel Estimation Error

The channel estimation accuracy can be improved by incorporating an iterative channel estimation scheme. How the mean squared estimation error (MSE) is reduced by the use of iterative channel estimation was evaluated by computer simulations. MSE is defined as

$$MSE = E[|\xi_{m,l}(g,n) - \tilde{\xi}^{(i)}_{m,l}(g,n)|^2]. \tag{9}$$

Figure 4 plots the MSE performance as a function of the average $E_b/N_0$ with the number of iterations as a parameter for a fast fading channel ($f_D T_{slot} = 0.32$). The first iteration stage uses adaptive prediction using SA or LI and the 2nd and later iteration stages use a $Q = 50$ moving average filtering. Figure 4 clearly shows the effectiveness of the use of iterative channel estimation. As the number of iterations increases, the value of MSE reduces; however, only slight additional reduction is obtained at the 4th iteration stage. In iterative channel estimation, tentative decision results are fedback as pilot symbols. In Fig. 4, the MSE curves labeled "perfect feedback" are for without feedback error. (The impact of feedback error is discussed in detail in Sect. 3.5.) It can be seen that the MSE at 3rd iteration approaches that of "perfect feedback". The above results imply that the BER performance may improves as

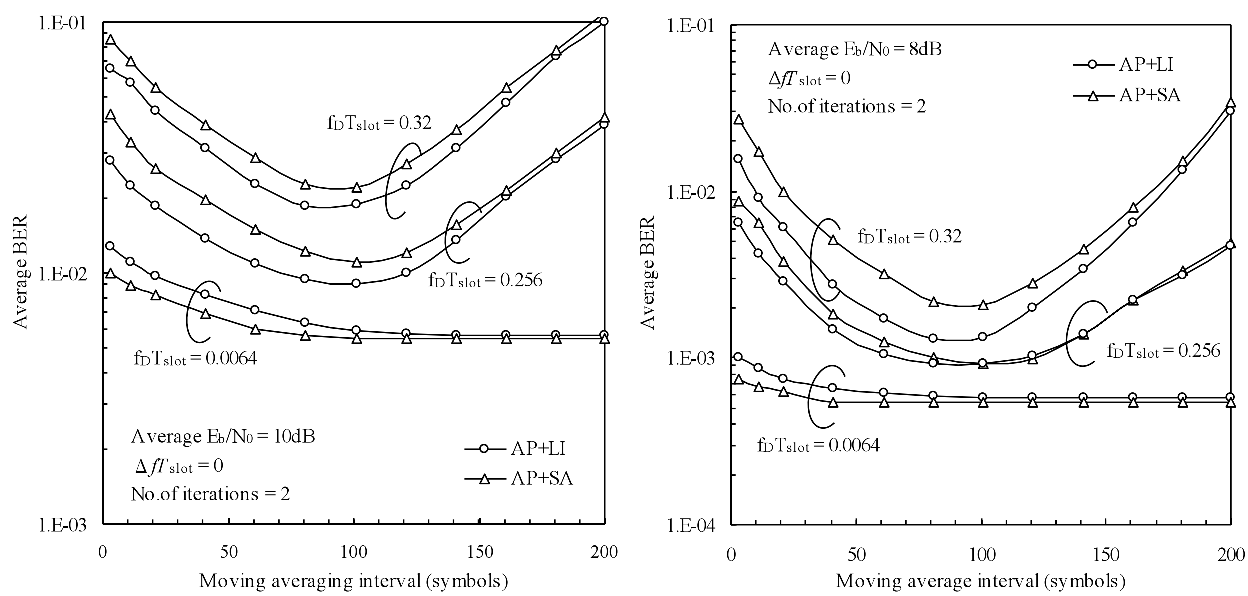


(a) Without diversity ($M = 1$) (b) With diversity ($M = 2$)

**Fig. 3** Effect of moving average interval ($2Q + 1$ symbols) for channel re-estimation in second and later iteration stages.

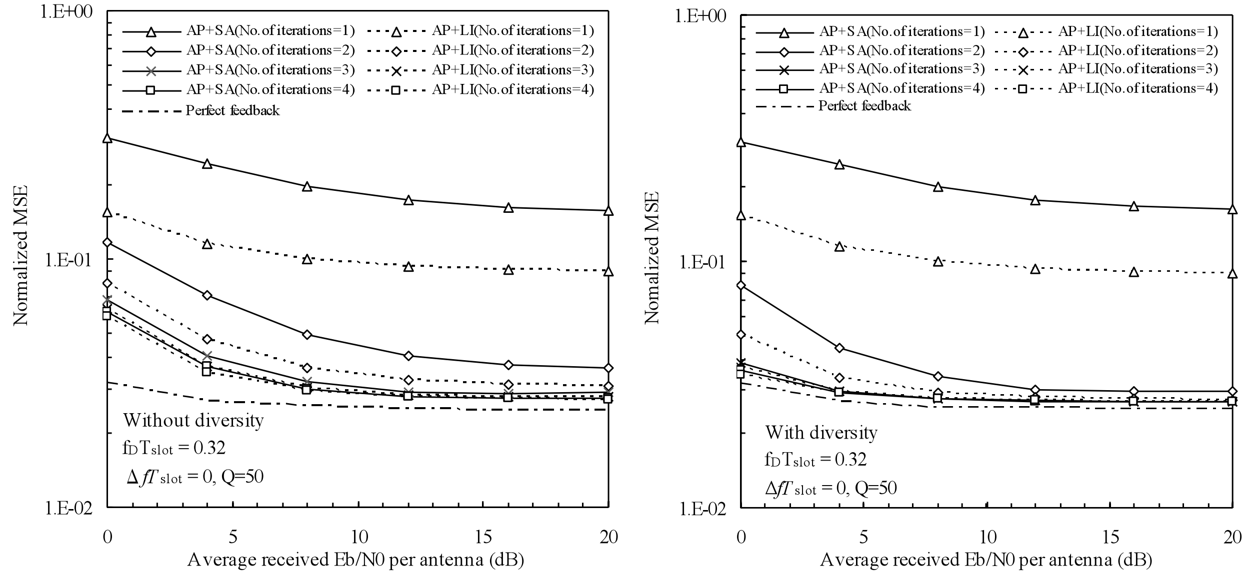


(a) Without diversity ($M = 1$) (b) With diversity ($M = 2$)

**Fig. 4** Effect of number of iterations on MSE for $f_D T_{slot} = 0.32$. SA and LI are used at the 1st stage.

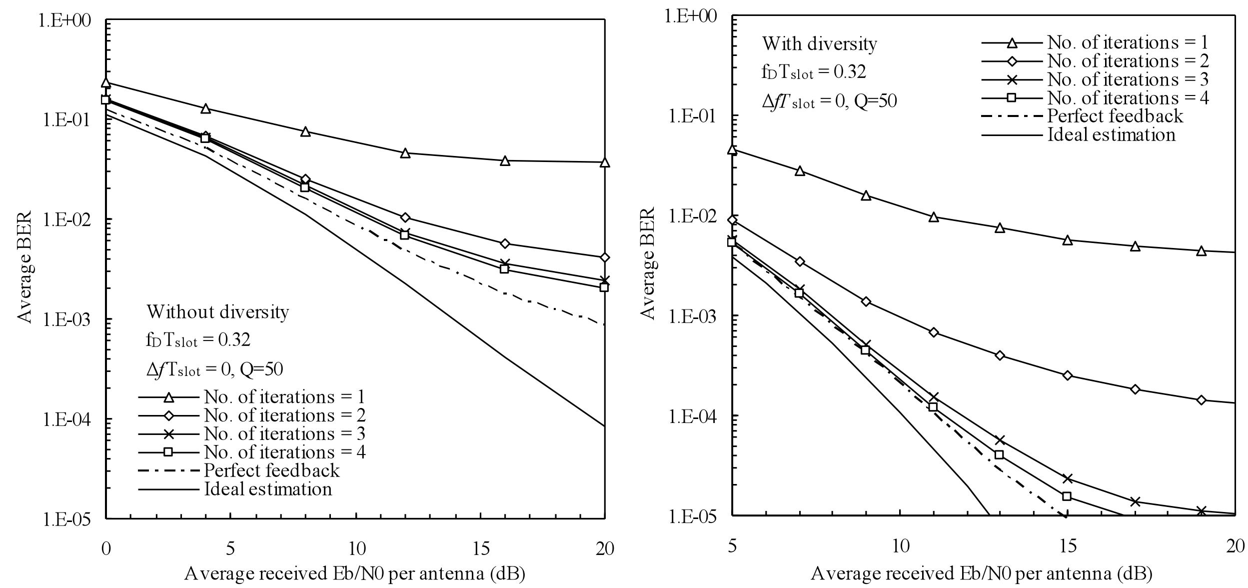


(a) Without diversity ($M = 1$) (b) With diversity ($M = 2$)

**Fig. 5** Effect of number of iterations on achievable BER performance for $f_D T_{slot} = 0.32$. SA is used at the 1st stage.

the number of iterations increases; however, the use of three iterations (including the first) may be sufficient.

### 3.4 Effect of Number of Iterations

Figure 5 plots the BER performance with the number of iterations as a parameter when $f_D T_{slot} = 0.32$. The first iteration stage uses adaptive prediction using SA and the 2nd and later iteration stages use a $Q = 50$ moving average filtering. It can be clearly seen that iterative channel estimation has a significant impact on reducing the BER performance and as the number of iterations increases, the BER performance approaches that of ideal channel estimation (the set of channel gains $\{\xi_{m,l}\}$ is perfectly known). With diversity reception, an $E_b/N_0$ degradation of as small as 0.8 dB is achieved at the 4th iteration stage for BER $= 10^{-3}$ (of which 0.28 dB $E_b/N_0$ degradation is due to pilot insertion loss). In low $E_b/N_0$ regions where the AWGN is the major cause of errors, the BER performance sig-

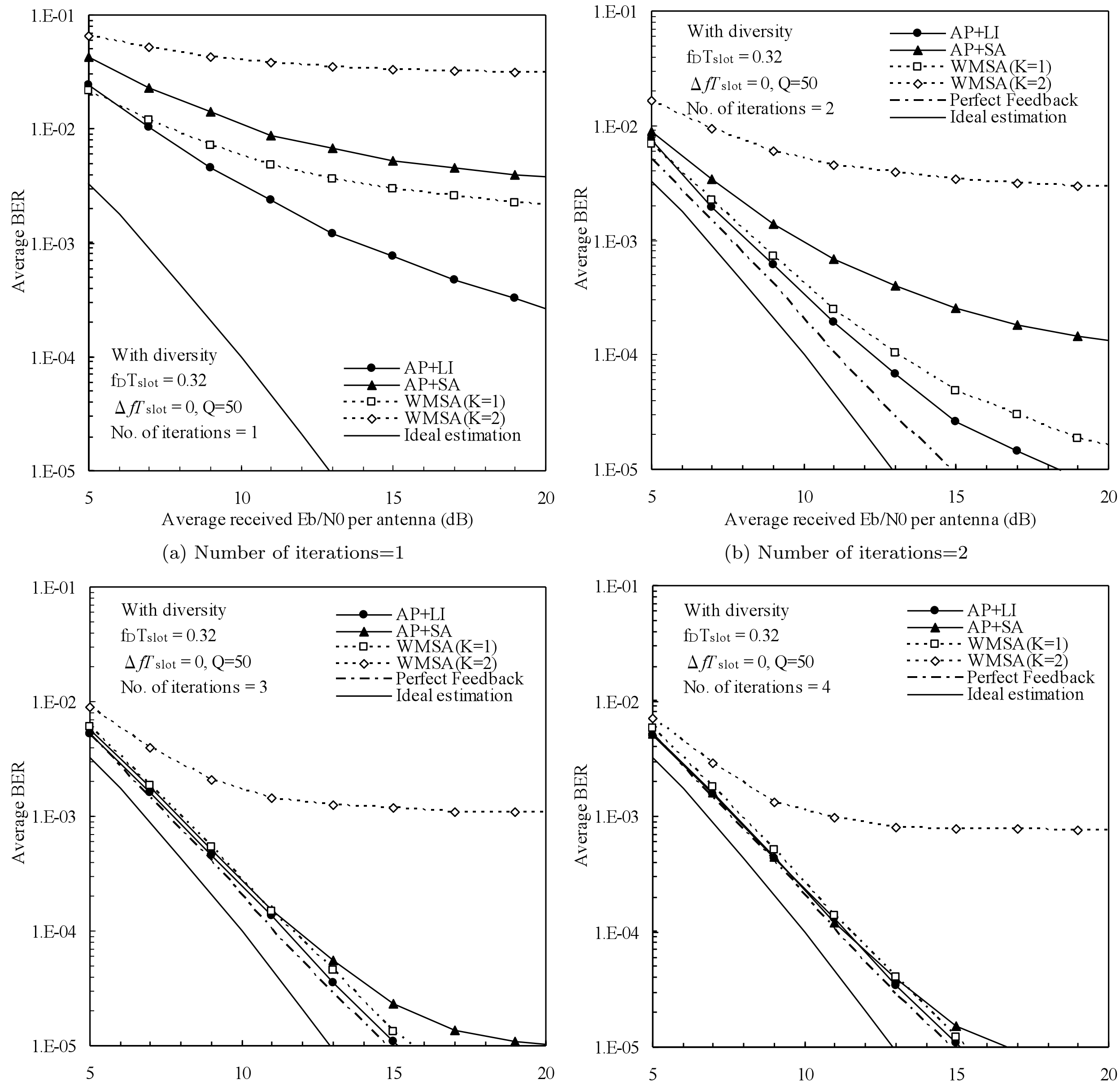


(a) Number of iterations=1

(b) Number of iterations=2

(c) Number of iterations=3

(d) Number of iterations=4

**Fig. 6** Average BER performance for various number of iterations as a function of the average received $E_b/N_0$ for $M = 2$ and $f_D T_{slot} = 0.32$.

nificantly improves at the 3rd iteration stage; however, almost no additional improvement is obtained at the 4th iteration stage as shown in Ref. [13]. Therefore, the use of three iterations is considered to be sufficient.

In high $E_b/N_0$ regions, the BER floor is observed. The use of iterative channel estimation is significant in reducing the BER floor. It is seen in Fig. 5 that, with antenna diversity, the BER floor is $8 \times 10^{-3}$ at the 1st iteration stage. This can reduce to $2 \times 10^{-4}$ and $1 \times 10^{-5}$ at the 2nd and the 3rd iteration stages, respectively. Only slight additional reduction in the BER floor is observed at the 4th iteration stage, as implied from Fig. 4.

### 3.5 Performance Comparison

The BER performances achievable by the adaptive prediction iterative channel estimation are compared with non-adaptive iterative channel estimation using conventional WMSA filter at the first iteration. Figure 6 plots the BER performances in a fast fading channel ($f_D T_{slot} = 0.32$) with the number of iterations as a parameter for diversity reception case ($M = 2$). Since non-adaptive iterative channel estimation using $K = 3$ WMSA (at the 2nd step of the 1st stage) cannot achieve BER floor of less than $10^{-3}$, its BER performance is not plotted in Fig. 6. WMSA channel estimation is designed to emphasize on reducing the noise effect at the cost of slightly losing the tracking ability against fading. Hence, non-adaptive iterative channel estimation using WMSA (in particular $K = 2$) do not perform well in a fast fading environment. It can be seen in Fig. 6 that the adaptive prediction iterative channel estimation can achieve better BER performance than non-adaptive iterative channel estimation using WMSA ($K = 1, 2$); however, the performance difference becomes smaller when the number of iterations becomes more than three.

In iterative channel estimation, tentative decision results are fedback as pilot symbols. Feeding back of decision errors limits the channel estimation accuracy. To see how the feedback errors affect the BER performance achievable by iterative channel estimation, the BER performance without feedback errors labeled "perfect feedback" is also plotted in Fig. 6. It can be seen that the BER performance at the 3rd iteration almost approaches that without feedback error and using AP+LI is found to provide the best performance among four schemes of AP+SA, AP+LI, WMSA ($K = 1$), and WMSA ($K = 2$). This is implied from Fig. 4.

In Fig. 6, the BER performance with ideal channel estimation case is also plotted for comparison. The BER performance with adaptive prediction iterative channel estimation approaches that with ideal channel estimation as the number of iterations increases, but there is still a performance gap. This is because the estimation error increases due to noise when the received signal fades in a slow fading and due to increasing prediction error for a fast fading environment. The latter can possibly be overcome by replacing a simple moving average filter of Eq. (8) by a prediction filter.

The causes of channel estimation errors are (a) feedback of decision errors and (b) insufficient tracking ability against fading. The proposed adaptive prediction channel estimation schemes have improved tracking ability against fading. The linear prediction filter tap weights are adaptively updated according to the change in fading environments. For a slow fading environment, the adaptive prediction filter acts as an averaging filter (i.e., the tap weights becomes almost the same) to emphasize on increasing the noise reduction. On the other hand, for a fast fading environment, the adaptive prediction filter emphasizes on predicting the fast varying complex channel gains at the cost of losing the noise reduction power. As clearly seen in Fig. 6, although the feedback errors affect the performance of iterative channel estimation, its effect can be made almost negligible if fading is not too fast (e.g., less than $f_D T_{slot}$ is 0.32). This is because the use of adaptive prediction filter can reduce the BER at the first stage compared to non-adaptive channel estimation, i.e., WMSA, and hence, reduced feedback errors achieve better BER performance.

Of course, the joint use of iterative channel estimation and error correction decoding can improve the BER performance because of less feedback errors. Since each iteration requires error correction decoding, the overall decoding delay increases. However, iterative channel estimation well matches the iterative decoding structure of turbo codes. Recently, the joint use of iterative channel estimation and turbo coding has been attracting much attention [17]. This study is out

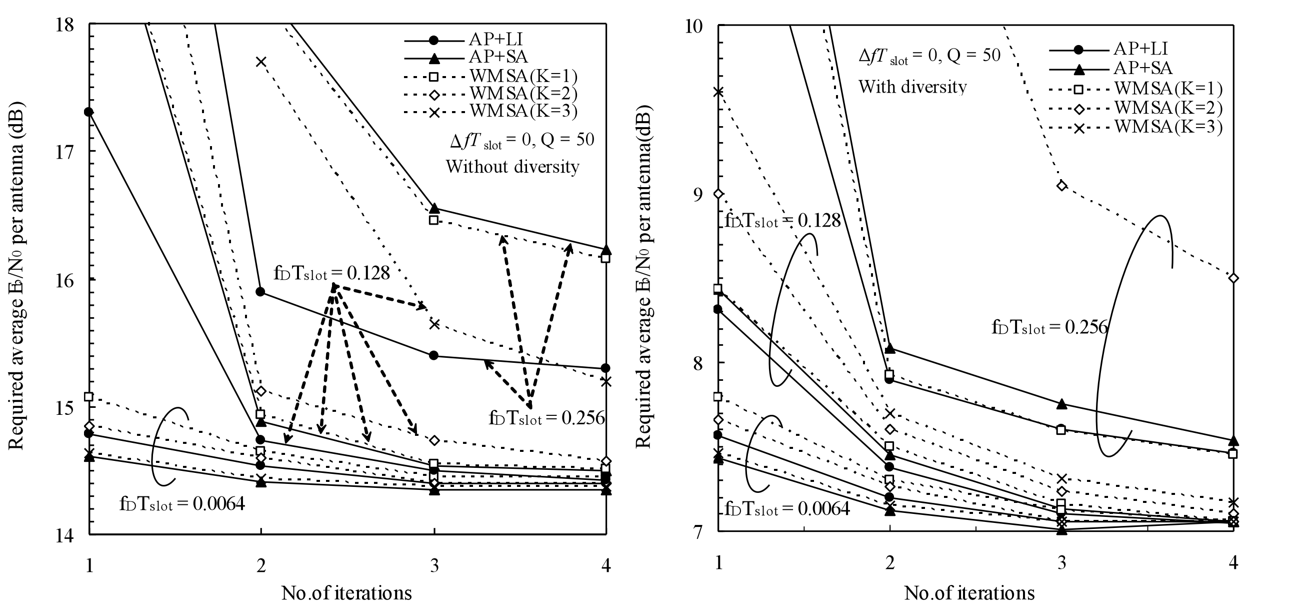


(a) Without diversity ($M = 1$)

(b) With diversity ($M = 2$)

**Fig. 7** Required $E_b/N_0$ for BER $= 10^{-3}$ with the value of $f_D T_{slot}$ as a parameter.

of scope of this paper and left for an interesting future research topic.

Figure 7 plots the required $E_b/N_0$ for BER $= 10^{-3}$ as a function of the number of iterations with the value of $f_D T_{slot}$ as a parameter. The comparison of SA and LI (used at the 3rd step of the 1st stage) in the adaptive prediction iterative channel estimation shows that the former provides better performance in a slow fading channel ($f_D T_{slot} = 0.0064$). In faster fading channels ($f_D T_{slot} = 0.128$ and $0.256$), however, adaptive prediction iterative channel estimation using LI provides better performance than using SA. With non-adaptive iterative channel estimation, the best performance is obtained using $K = 3$ WMSA in a slow fading channel but using $K = 1$ WMSA in a fast fading channel. Notice that the use of $K = 2$ and 3 WMSA in non-adaptive iterative channel estimation shows significant degradations in the performance in the fast fading channel (non-adaptive iterative channel estimation using $K = 3$ WMSA cannot achieve BER $= 10^{-3}$ in the fast fading of $f_D T_{slot} = 0.256$). Although, in the slow fading channel, the adaptive prediction iterative channel estimation using LI is inferior to the non-adaptive iterative channel estimation using $K = 3$ WMSA, the performance difference is very small. As a consequence, the adaptive prediction iterative channel estimation us-

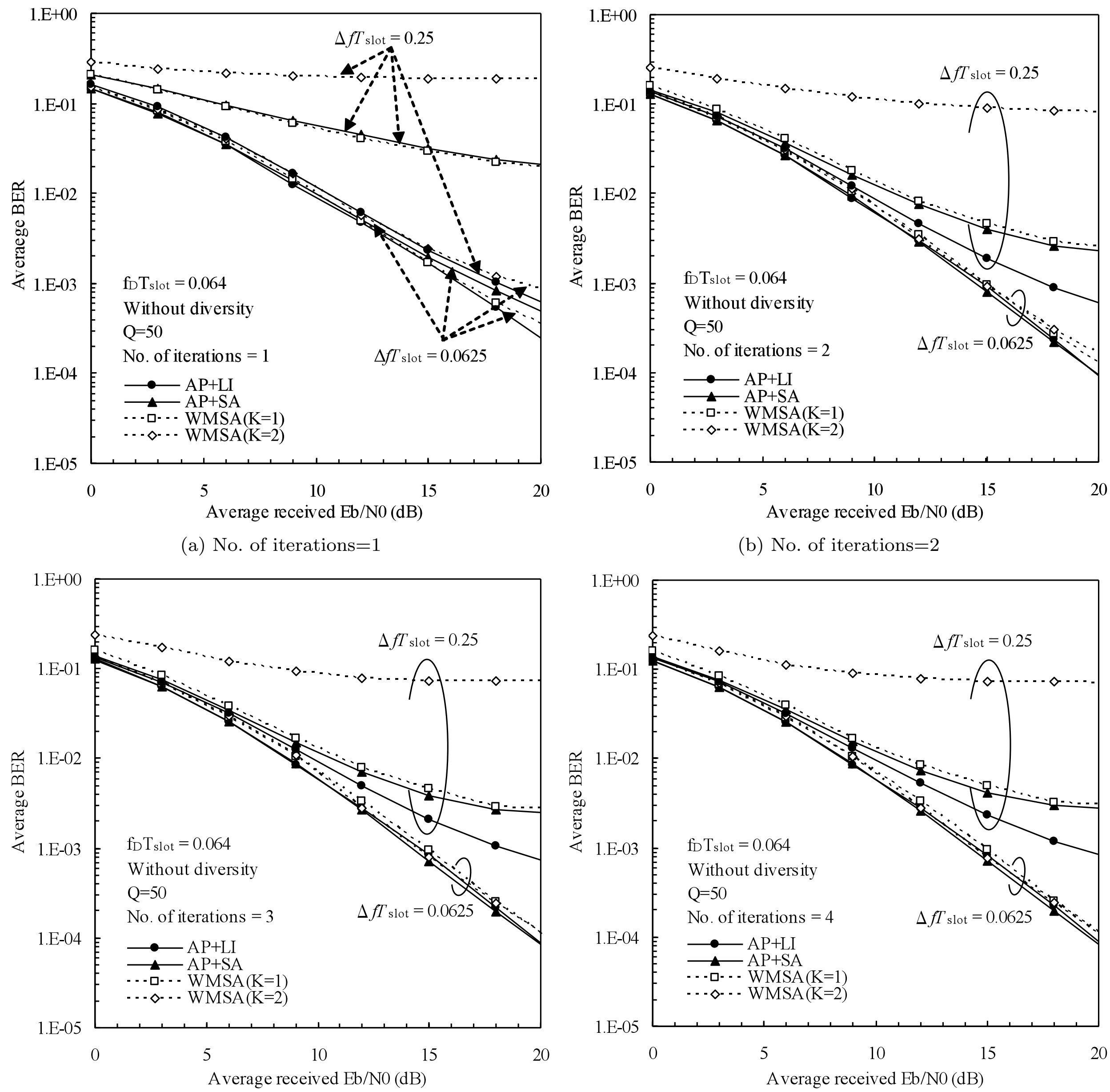


(a) No. of iterations=1

(b) No. of iterations=2

(c) No. of iterations=3

(d) No. of iterations=4

**Fig. 8** Average BER performance in the presence of frequency offset of $\Delta f T_{slot} = 0.0625$ and $0.25$ for $f_D T_{slot} = 0.064$ and no diversity ($M = 1$).

ing LI provides overall superior performance to the non-adaptive iterative channel estimation in slow-to-fast fading channels.

### 3.6 Impact of Frequency Offset between Transmitter and Receiver

When the frequency offset $\Delta f$ between the transmitter and receiver exists, the MF output $r_{m,l}(g,n)$ given by Eq. (5) can be rewritten as

$$r_{m,l}(g,n) = \sqrt{2S}\xi'_{m,l}(g,n)\exp[j\phi(g,n)] + w_{m,l}(g,n), \tag{10}$$

where $\xi'_{m,l}(g,n)$ represents the complex channel gain containing the effect of frequency offset $\Delta f$ and is given by

$$\xi'_{m,l}(g,n) = \xi_{m,l}(g,n)\exp[j2\pi\Delta f(gT_{slot}+nT)]. \tag{11}$$

It can be understood that the multipath fading produces the random phase variations, but the frequency offset produces the constant phase rotation. The adaptive prediction channel estimation scheme proposed in this paper can estimate $\xi'_{m,l}(g,n)$. The average BER performance degrades due to the frequency offset as well as fading. How the proposed channel estimation scheme improves the average BER performance is evaluated by computer simulations. The simulation results are plotted in Figs. 8 and 9. To see clearly the effect of adaptive prediction channel estimation in the presence of frequency offset, we consider no diversity ($M = 1$) case only.

Figure 8 plots the BER performance in the presence of the frequency offset when the normalized frequency offset $\Delta fT_{slot} = 0.0625$ and 0.25 (i.e., $\Delta fT =$ 0.000977 and 0.00391). When $\Delta fT_{slot} = 0.0625$, the impact of the frequency offset is very small and iterative channel estimation can almost completely remove the effect of frequency offset. On the other hand, when $\Delta fT_{slot} = 0.25$, the BER performance is significantly degraded if adaptive prediction iterative channel estimation is not used. As discussed in Sect. 3.4, the use of three iterations is considered to be sufficient to reduce the effect of frequency offset. Adaptive prediction channel estimation using SA and LI (used at the 3rd step of the 1st iteration stage) provides better performance than non-adaptive channel estimation using WMSA.

Figure 9 plots the BERs with and without iterative channel estimation (the number of iterations=1 and 3, respectively) at the average $E_b/N_0 = 20$ dB as a function of $\Delta fT_{slot}$ for $f_DT_{slot} = 0.064$. For the small values of $\Delta fT_{slot}$ below about 0.05, the predominant cause of decision errors is the AWGN and hence, the BER is almost constant. However, as $\Delta fT_{slot}$ increases beyond 0.05, the BER starts to increase due to the rapid phase rotation due to the frequency offset. However, it can be clearly seen that the use of adaptive iterative channel estimation using SA and LI (used at the 3rd step of the 1st iteration stage) significantly reduces the BER produced by the frequency offset; using LI is found to provide overall the best performance.

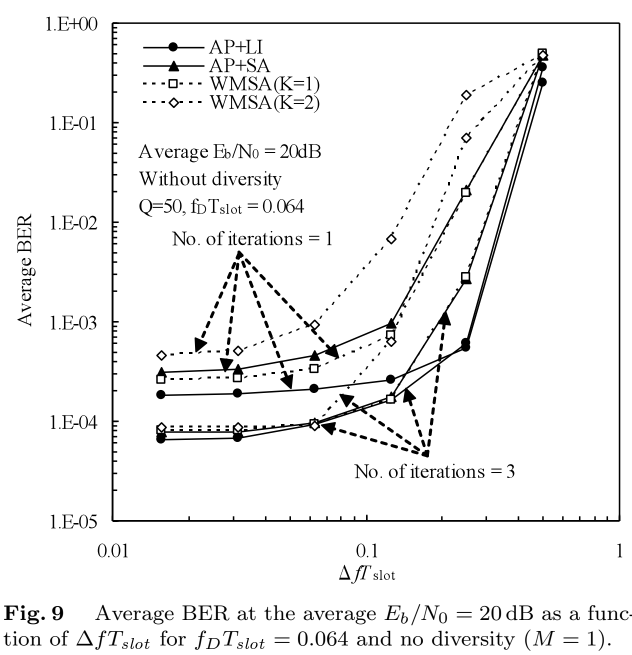


**Fig. 9** Average BER at the average $E_b/N_0 = 20$ dB as a function of $\Delta fT_{slot}$ for $f_DT_{slot} = 0.064$ and no diversity ($M = 1$).

## 4. Conclusion

Adaptive prediction iterative channel estimation was presented for combined antenna diversity and coherent rake reception of DSSS signals. The first iteration stage uses a pilot-aided adaptive prediction and the second and later iteration stages use decision-feedback and moving average filtering for channel re-estimation. The computer simulation confirmed that, as the number of iterations increases, the BER performance significantly improves and approaches that of ideal channel estimation. In the low $E_b/N_0$ regions, the use of three iterations (including the first) is sufficient. The use of iterative channel estimation is even significant in reducing the BER floor observed in high $E_b/N_0$ regions. This is also true in the presence of frequency offset between the transmitter and receiver in addition to multipath fading. It is also found that the choice of first stage channel estimation method does not affect much the resultant BER performance if the number of iterations is more than three. However, the adaptive prediction iterative channel estimation using linear interpolation (LI) provides overall superior performance to non-adaptive iterative channel estimation in slow-to-fast fading channels.

In this paper we did not consider channel coding. Iterative channel estimation well matches the iterative decoding structure of turbo codes. The joint use of iterative channel estimation and turbo coding has been attracting much attention [17]. This is left for an interesting future research topic. As seen in Fig. 6, there is a performance gap between the achievable BER performance with adaptive prediction iterative channel estimation and with ideal channel estimation. The gap may be able to narrow by replacing a simple moving average filter of Eq. (8) by a prediction filter. This is also left for a future study.

**References**


[1] W.C. Jakes, Jr., ed., Microwave mobile communications, Wiley, New York, 1974.

[2] F. Ling, "Coherent detection with reference-symbol based estimation for direct sequence CDMA uplink communications," Proc. IEEE Veh. Technol. Conf., pp.400–403, May 1993.

[3] S. Sampei and T. Sunaga, "Rayleigh fading compensation for QAM in land mobile radio communication," IEEE Trans. Veh. Technol., vol.42, pp.137–147, May 1993.

[4] C.I. Bang and M.H. Lee, "An analysis of pilot symbol assisted 16QAM in the Rayleigh fading channel," IEEE Trans. Consum. Elect., vol.41, pp.1138–1141, Nov. 1995.

[5] H. Andoh, M. Sawahashi, and F. Adachi, "Channel estimation filter using time-multiplexed pilot channel for coherent RAKE combining in DS-CDMA mobile radio," IEICE Trans. Commun., vol.E81-B, no.7, pp.1517–1526, July 1998.

[6] Y. Honda and K. Jamal, "Channel estimation based on time-multiplexed pilot symbols," IEICE Technical Report, RCS96-70, Aug. 1996.

[7] S. Abeta, M. Sawahashi, and F. Adachi, "Adaptive channel estimation for coherent DS-CDMA mobile radio using time-multiplexed pilot and parallel pilot structure," IEICE Trans. Commun., vol.E82-B, no.9, pp.1505–1513, Sept. 1999.

[8] S. Takaoka and F. Adachi, "Adaptive predictive channel estimation using time-multiplexed pilot symbols in a multipath fading channel," Transmission Engineering Technical Meeting, no.441, Tohoku University, 16 May 2001.

[9] F. Adachi, "BER analysis of 2PSK, 4PSK, and 16QAM with decision feedback channel estimation in frequency-selective slow Rayleigh fading," IEEE Trans. Veh. Technol., vol.48, no.9, pp.1563–1572, Sept. 1999.

[10] A. Zhuang and M. Renfors, "Combined pilot aided and decision directed channel estimation for the RAKE receiver," Proc. IEEE Veh. Technol. Conf., vol.2, pp.710–713, Sept. 2000.

[11] M. Sawahashi, Y. Miki, H. Andoh, and K. Higuchi, "Pilot symbol-assisted coherent multistage interference canceller using recursive channel estimation for DS-CDMA mobile radio," IEICE Trans. Commun., vol.E79-B, no.9, pp.1262–1270, Sept. 1996.

[12] M. Sawahashi, H. Andoh, and K. Higuchi, "Interference rejection weight control for pilot symbol-assisted coherent multistage interference canceller using recursive channel estimation in DS-CDMA mobile radio," IEICE Trans. Fundamentals, vol.E81-A, no.5, pp.957–972, May 1998.

[13] K. Okawa, K. Higuchi, and M. Sawahashi, "Parallel-type coherent multi-stage interference canceller with iterative channel estimation using both pilot and decision-feedback data symbols for W-CDMA mobile radio," IEICE Trans. Commun., vol.E84-B, no.3, pp.446–456, March 2001.

[14] G.M. Vitetta and D.P. Taylor, "Maximum likelihood decoding of uncoded and coded PSK signal sequences transmitted over Rayleigh flat-fading channels," IEEE Trans. Commun., vol.43, pp.2750–2758, Nov. 1995.

[15] S. Haykin, Adaptive Filter Theory, 3rd ed., Prentice Hall, Englewood Cliffs, NJ, 1996.

[16] C. Kchao and G.L. Stuber, "Analysis of a direct-sequence spread-spectrum cellular radio system," IEEE Trans. Commun., vol.41, pp.1507–1516, Oct. 1993.

[17] M.C. Valenti, "Iterative channel estimation and decoding of pilot symbol assisted turbo codes over flat-fading channels," IEEE J. Sel. Areas Commun., vol.19, no.9, pp.1694–1705, Sept. 2001.


## Appendix: Adaptive Prediction Channel Estimation

Figure A· 1 illustrates the structure of pilot-aided adaptive prediction channel estimation, which consists of 3 steps [8]. In the first step, the instantaneous channel gain is estimated by coherent addition of $N_p$ received pilot symbols after removing pilot phase. Without loss of generality, the pilot symbol phase of $\phi = \pi/4$ is assumed. The instantaneous channel estimate, $\hat{\xi}_{m,l}(g)$, at the beginning of the $g$th slot is given by

$$\hat{\xi}_{m,l}(g) = \frac{1}{N_p} \sum_{n=0}^{N_p-1} r_{m,l}(g,n) \exp(-j\pi/4). \qquad (\text{A}\cdot 1)$$

Then, the second step predicts the instantaneous channel gains, $\tilde{\xi}_{m,l,f}(g)$ and $\tilde{\xi}_{m,l,b}(g)$, at the end of and beginning of data slot by a forward predictor and backward predictor using the $K$ past and $K$ future instantaneous channel gains, $\{\hat{\xi}_{m,l}(g)\}$, respectively. The tap weights of forward predictor and backward predictor are adaptively updated using the normalized LMS algorithm [15]. $\tilde{\xi}_{m,l,f}(g)$ and $\tilde{\xi}_{m,l,b}(g)$ are given by

$$\begin{cases} \tilde{\xi}_{m,l,f}(g) = \boldsymbol{W}_{m,l,f}(g)\boldsymbol{X}^T_{m,l,f}(g) \\ \tilde{\xi}_{m,l,b}(g) = \boldsymbol{W}_{m,l,b}(g)\boldsymbol{X}^T_{m,l,b}(g) \end{cases} \qquad (\text{A}\cdot 2)$$

with

$$\begin{cases} \boldsymbol{W}_{m,l,f}(g) = [w_{m,l,0}(g), w_{m,l,-1}(g), \\ \quad \cdots, w_{m,l,-K+1}(g)] \\ \boldsymbol{X}_{m,l,f}(g) = [\hat{\xi}_{m,l}(g), \hat{\xi}_{m,l}(g-1), \\ \quad \cdots, \hat{\xi}_{m,l}(g-K+1)] \end{cases}, \qquad (\text{A}\cdot 3\text{a})$$

$$\begin{cases} \boldsymbol{W}_{m,l,b}(g) = [w_{m,l,1}(g), w_{m,l,2}(g), \\ \quad \cdots, w_{m,l,K}(g)] \\ \boldsymbol{X}_{m,l,b}(g) = [\hat{\xi}_{m,l}(g+1), \hat{\xi}_{m,l}(g+2), \\ \quad \cdots, \hat{\xi}_{m,l}(g+K)] \end{cases}, \qquad (\text{A}\cdot 3\text{b})$$

where $[.]^T$ denotes transpose, $\boldsymbol{W}_{m,l,f}(g)$ and $\boldsymbol{W}_{m,l,b}(g)$ are respectively the complex tap weight vectors for the forward and backward predictions, and $\boldsymbol{X}_{m,l,f}(g)$ and $\boldsymbol{X}_{m,l,b}(g)$ are respectively the vectors of estimated instantaneous channel gains used for the forward and backward predictors.

The tap weight vectors, $\boldsymbol{W}_{m,l,f}(g)$ and $\boldsymbol{W}_{m,l,b}(g)$ are updated based on the normalized LMS algorithm

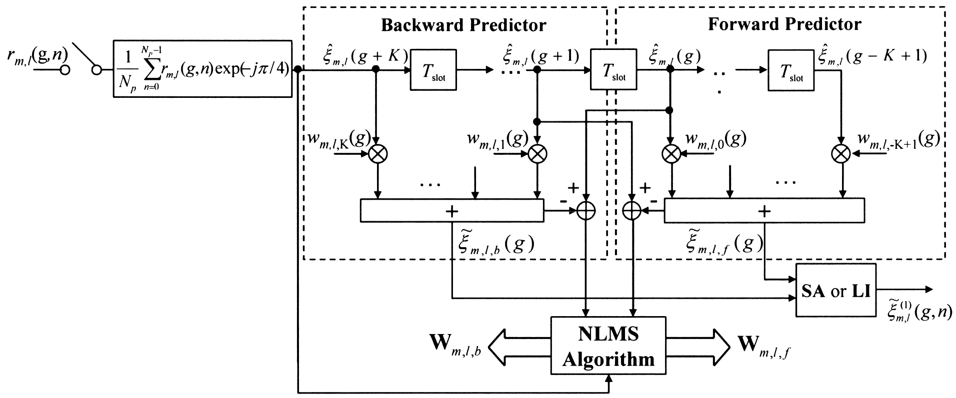


**Fig. A·1** Adaptive prediction in the first iteration stage.

[15] using $\hat{\xi}_{m,l}(g{+}1)$ and $\hat{\xi}_{m,l}(g)$ as the reference signals:

$$\begin{cases} \boldsymbol{W}_{m,l,f}(g+1) = \boldsymbol{W}_{m,l,f}(g) \\ \quad +\mu \dfrac{e_{m,l,f}(g)}{\sum_{j=0}^{K-1} |\hat{\xi}_{m,l}(g-j)|^2} \boldsymbol{X}^*_{m,l,f}(g) \\ e_{m,l,f}(g) = \hat{\xi}_{m,l}(g+1) - \tilde{\xi}_{m,l,f}(g) \end{cases}, \tag{A·4a}$$

$$\begin{cases} \boldsymbol{W}_{m,l,b}(g+1) = \boldsymbol{W}_{m,l,b}(g) \\ \quad +\mu \dfrac{e_{m,l,b}(g)}{\sum_{j=1}^{K} |\hat{\xi}_{m,l}(g+j)|^2} \boldsymbol{X}^*_{m,l,b}(g) \\ e_{m,l,b}(g) = \hat{\xi}_{m,l}(g) - \tilde{\xi}_{m,l,b}(g) \end{cases}, \tag{A·4b}$$

where $e_{m,l,f}(g)$ and $e_{m,l,b}(g)$ are the estimation errors and $\mu$ is the step size.

Finally, in the third step, the instantaneous channel gain, $\tilde{\xi}_{m,l}(g,n)$, at the $n$th data symbol position of the $g$th data slot is estimated by simple averaging (SA) or linear interpolation (LI) using the two adaptively predicted instantaneous channel gains of $\tilde{\xi}_{m,l,b}(g)$ and $\tilde{\xi}_{m,l,f}(g)$. Then, $\tilde{\xi}^{(1)}_{m,l}(g,n)$, for $n = N_p \sim N_p + N_d - 1$, is given by

SA:

$$\tilde{\xi}^{(1)}_{m,l}(g,n) = \frac{\tilde{\xi}_{m,l,f}(g) + \tilde{\xi}_{m,l,b}(g)}{2} \tag{A·5a}$$

LI:

$$\begin{aligned} \tilde{\xi}^{(1)}_{m,l}(g,n) = & \frac{\left(n - \dfrac{N_p-1}{2}\right)}{N_p + N_d} \tilde{\xi}_{m,l,f}(g) \\ & + \left\{ 1 - \frac{\left(n - \dfrac{N_p-1}{2}\right)}{N_p + N_d} \right\} \tilde{\xi}_{m,l,b}(g). \end{aligned} \tag{A·5b}$$

In the computer simulations, we use $K = 4$ and the step size $\mu = 0.01$.

**Shinsuke Takaoka** received his B.S. degree in communications engineering from Tohoku University, Sendai, Japan, in 2001. Currently, he is a graduate student at the Department of Electrical and Communications Engineering, Tohoku University. His research interests include wireless digital siginal transmission techniques, especially for mobile communications systems.

**Fumiyuki Adachi** received his B.S. and Dr.Eng. degrees in electrical engineering from Tohoku University, Sendai, Japan, in 1973 and 1984, respectively. In April 1973, he joined the Electrical Communications Laboratories of Nippon Telegraph & Telephone Corporation (now NTT) and conducted various types of research related to digital cellular mobile communications. From July 1992 to December 1999, he was with NTT Mobile Communications Network, Inc. (now NTT DoCoMo, Inc.), where he led a research group on wideband/broadband CDMA wireless access for IMT-2000 and beyond. Since January 2000, he has been with Tohoku University, Sendai, Japan, where he is a Professor of Electrical and Communication Engineering at Graduate School of Engineering. His research interests are in CDMA and TDMA wireless access techniques, CDMA spreading code design, Rake receiver, transmit/receive antenna diversity, adaptive antenna array, bandwidth-efficient digital modulation, and channel coding, with particular application to broadband wireless communications systems. From October 1984 to September 1985, he was a United Kingdom SERC Visiting Research Fellow in the Department of Electrical Engineering and Electronics at Liverpool University. From April 1997 to March 2000, he was a visiting Professor at Nara Institute of Science and Technology, Japan. He was a co-recipient of the IEICE Transactions best paper of the year award 1996 and again 1998. He is an IEEE Fellow and was a co-recipient of the IEEE Vehicular Technology Transactions best paper of the year award 1980 and again 1990 and also a recipient of Avant Garde award 2000.